



# Extreme learning machine-based super-twisting repetitive control for aperiodic disturbance, parameter uncertainty, friction, and backlash compensations of a brushless DC servo motor

Raymond Chuei<sup>1</sup> · Zhenwei Cao<sup>1</sup>

Received: 26 February 2019 / Accepted: 18 April 2020  
© Springer-Verlag London Ltd., part of Springer Nature 2020

## Abstract

This paper presents an extreme learning machine-based super-twisting repetitive control (ELMSTRC) to improve the tracking accuracy of periodic signal with less chattering. The proposed algorithm is robust against the plant uncertainties caused by mass and viscous friction variations. Moreover, it compensates the nonlinear friction and the backlash by using extreme learning machine based super-twisting algorithm. Firstly, a repetitive control is designed to track the periodic reference and compensate the viscous friction. Then, a stable extreme learning machine-based super-twisting control is constructed to compensate the aperiodic disturbance, nonlinear friction, backlash and plant uncertainties. The stability of ELMSTRC system is analysed based on Lyapunov stability criteria. The proposed algorithm is verified on a brushless DC servo motor with various loading, backlash and friction conditions. The simulation and experimental comparisons highlight the advantages of the proposed algorithm.

**Keywords** Aperiodic disturbance · Backlash · Chattering · Coulomb friction · Extreme learning machine · Neural network · Nonlinear control · Parameter uncertainty · Periodic signal · Repetitive control · Super-twisting control · Viscous friction

## 1 Introduction

Repetitive control (RC) was firstly proposed by Inoue et al. [1] in 1980s based on the internal model principle [2] to track the periodic signals and reject the periodic disturbances. RC can be applied on hard disk drives, robot manipulators, induction motors, power electronic devises, and more. Hence, RC has been studied by many scholars recently [3–7]. However, the conventional RC system is a neutral-type delay system. It may cause the whole system unstable, since the plant is strictly proper in most of the engineering applications. Hence, Hara et al. [3] proposed a modified RC (MRC) which inserts a low-pass filter in the delay line to stabilise the strictly proper plant.

There is a limitation that RC cannot compensate and may even amplify the aperiodic disturbances [7]. Hence, the integration of RC with sliding mode control (SMC) is necessary, since the SMC is robust against aperiodic disturbances, and parameter variations [8–10]. However, the SMC produces undesired chattering due to the nonlinearity of the sign function. In order to reduce the chattering, the super-twisting control (STC) algorithm [11] was applied on super-twisting-based repetitive control (STRC) [12], which requires only information of the system output and achieves the finite-time convergence of the sliding variable.

In addition, the nonlinearities such as deadzone, backlash, and friction are the main concerns in most of the rotational systems. Backlash is a clearance or lost motion in a machine caused by gaps between the adjacent movable parts [13]. Nonlinear friction or Coulomb friction is a kind of resistance force generated by the relative motion of the two surfaces [14]. The backlash and nonlinear friction may cause the energy loss and reduce the tracking performance of the control systems. Furthermore, the parameter

---

✉ Raymond Chuei  
rchuei@swin.edu.au

<sup>1</sup> Faculty of Science, Engineering and Technology, Swinburne University of Technology, Melbourne, Australia

uncertainties such as variation of load or friction coefficient reduce the tracking accuracy and cause the system unstable [15].

Hence, a series of adaptive control algorithms has been developed to compensate the uncertainties of nonlinear systems [16–18]. The describing function [13] is used to design a linear robust control to compensate the nonlinearities of the system, which is not effective for time-varying backlash and friction. Li et al. [17] proposed an adaptive fuzzy control to compensate the backlash-like hysteresis of simple pendulum system. However, the stability analysis of fuzzy control is complicated. Furthermore, the controller requires many tuning parameters in the design process.

The neural network (NN) system has been recently applied on dynamic control due to its strong estimating ability [19–22]. In [19, 20], a radial basic function neural network (RBFNN) is applied to compensate the uncertainty of nonlinear dynamic systems. However, a large number of tuning parameters increases the computational time and complexity of NN. Support vector machine (SVM) [23] is a powerful learning tool to estimate the uncertainty effectively. But there is a trade-off between the learning speed and estimating accuracy during the optimising process. Extreme learning machine (ELM) [24] is constructed by a novel single hidden layer feedforward neural network (SLFN). During the learning process, the input weights and input biases of ELM are set randomly, and only the output weights are tuned by the adaptive law. The learning process is simple and fast. Therefore, ELM is the ideal algorithm for estimating and compensating the uncertainty in real time.

ELM has been widely applied in many control applications. [25] applied ELM to compensate the system uncertainties of inverted pendulum system. A ELM-based single-layer-feedback neural networks identifier was proposed by Yang et al. [26] to compensate the nonlinearities, plant parameter variations, and external disturbances of power transmission line deicing robot. Yang et al. [27] integrated ELM into the haptic identifier to compensate the unknown nonlinearity of robot manipulator. In [28], ELM was used to compensate the unknown lumped uncertainty of electronic throttle.

In this paper, the proposed extreme learning machine based super-twisting repetitive control (ELMSTRC) firstly integrates ELM and STC algorithms to obtain extreme learning machine based super-twisting control (ELMSTC) and then combines the features of RC to further improve the tracking performance of periodic signals. The contributions of the proposed controller are highlighted as follows: (1) The RC in the proposed controller can track the periodic references precisely and compensate the viscous friction. (2) The STC in the proposed controller can ensure

finite-time convergence of sliding trajectory with less chattering under system uncertainties. (3) The ELM algorithm in the proposed controller can estimate and compensate the aperiodic disturbance, nonlinear friction, backlash, and parameter uncertainty efficiently. Furthermore, the boundary of the lumped uncertainty is not necessary.

The paper is organised as follows: Sect. 2 describes the plant model. Section 3 illustrates the design of ELMSTRC. Section 4 presents the simulations and comparison studies, Sect. 5 conducts the experiments and comparison studies, and Sect. 6 presents the conclusions of the paper.

In this paper,  $t$  is time variable;  $s$  is complex frequency variable.

## 2 Plant modelling

In Fig. 1, a nonlinear second-order dynamic model of a brushless DC servo motor is considered

$$\ddot{x}(t) = f(x(t)) + g(x(t))[u(t) + d(t)] \quad (1)$$

where  $u(t)$ ,  $x(t)$ ,  $\dot{x}(t)$  and  $\ddot{x}(t)$  are the control input, output position, output velocity and output acceleration, respectively.  $d(t)$  is external disturbance where  $|d(t)| \leq \Delta_d$ .  $f(x(t))$  and  $g(x(t))$  are unknown nonlinear functions where  $|f(x(t))| \leq \Delta_f$  and  $|g(x(t))| \leq \Delta_g$ .

Equation (1) can be rewritten as

$$\begin{aligned} \ddot{x}(t) &= f_o(x(t)) + \Delta f(x(t)) \\ &\quad + [g_o + \Delta g(x(t))][u(t) + d(t)] \\ &= f_o(x(t)) + g_o u(t) + d_{\text{lump}}(x(t)) \end{aligned} \quad (2)$$

where  $f_o(x(t))$  is known nominal linear function and  $g_o$  is known nominal input gain.  $\Delta f(x(t))$  and  $\Delta g(x(t))$  are unknown uncertainties. Hence, the lump uncertainty can be expressed as

$$d_{\text{lump}}(x(t)) = \Delta f(x(t)) + \Delta g(x(t))u(t) + g(x(t))d(t). \quad (3)$$

## 3 Design of extreme learning machine-based super-twisting repetitive control (ELMSTRC)

The proposed ELMSTRC system is shown in Fig. 1, which consists of nonlinear plant, RC, and ELMSTC.

The tracking error is defined as

$$e(t) = x(t) - r(t) \quad (4)$$

where  $e(t)$  and  $r(t)$  are the position error and reference position, respectively.

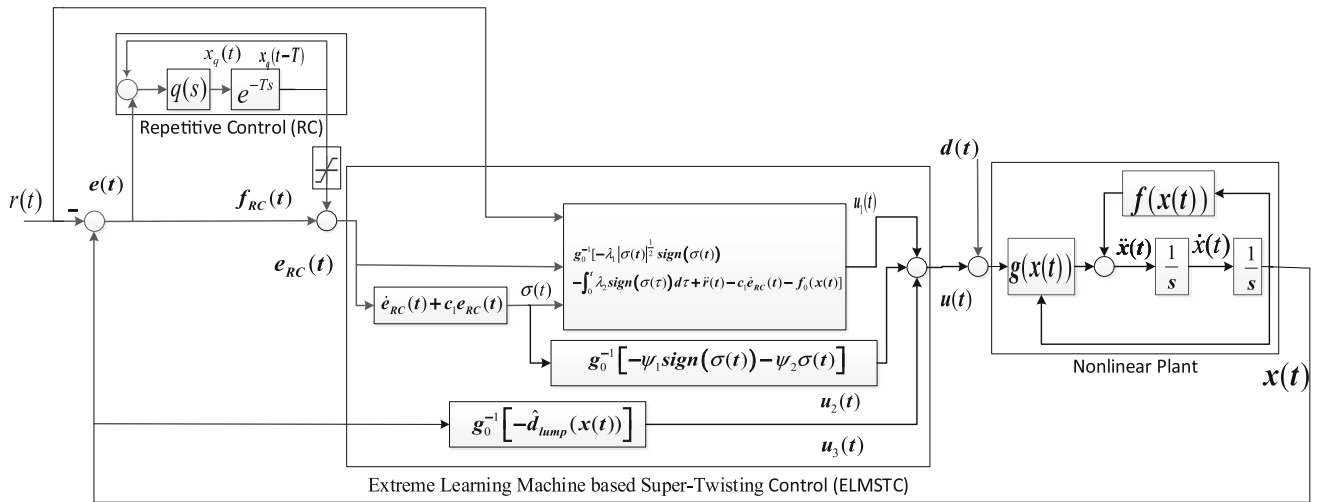


**Fig. 1** Structure of extreme learning machine-based super-twisting repetitive control (ELMSTC) system

### 3.1 Design of repetitive control (RC)

A modified RC [3] is cascaded with ELMSTC to track and compensate the periodic signals. RC can be designed as the following with time delay  $T_p$ , which is chosen as period of periodic signal  $r(t)$ .

$$C_{RC}(s) = \frac{q(s)e^{-sT_p}}{1 - q(s)e^{-sT_p}} \quad (5)$$

A first-order low-pass filter  $q(s)$  is designed as follows to stabilise the RC system

$$q(s) = \frac{\omega_q}{s + \omega_q} \quad (6)$$

The cut-off frequency  $\omega_q$  of the low-pass filter  $q(s)$  is tuned so that

$$\begin{cases} |q(j\omega)| \approx 1, & \omega \leq \omega_q \\ |q(j\omega)| < 1, & \omega > \omega_q \end{cases} \quad (7)$$

where  $\omega_q$  is the maximum cut-off frequency for the compensation of periodic signals [3, 29].

The state-space equation of RC can be expressed as

$$\dot{x}_q(t) = -\omega_q x_q(t) + \omega_q x_q(t - T_p) + \omega_q e(t) \quad (8)$$

A saturation function after RC is as follows:

$$\text{sat}[x_q(t - T_p)] = \begin{cases} x_q(t - T_p) & \text{if } x_q(t - T_p) \in [-\Delta_q, \Delta_q] \\ \Delta_q & \text{if } x_q(t - T_p) > \Delta_q \\ -\Delta_q & \text{if } x_q(t - T_p) < -\Delta_q \end{cases} \quad (9)$$

where  $t \geq 0$ .

Therefore, the RC compensated error signal is

$$e_{RC}(t) = e(t) + \text{sat}[x_q(t - T_p)] = e(t) + f_{RC}(t) \quad (10)$$

**Remark 1** The cut-off frequency  $\omega_q$  in the low-pass filter  $q(s)$  of RC is tuned to compensate the periodic signals. So that the periodic reference signals can be tracked accurately, and the periodic disturbances including viscous friction can be rejected effectively. Then, the tracking error  $e$  will converge to zero.

### 3.2 Design of ELM-based neural network

After this section,  $(t)$  is abbreviated for simplicity.

Firstly, single-layer feedforward network (SLFN) [24] is considered. For  $N$  arbitrary distinct samples  $(\mathbf{x}_i, \tau_i)$ , where  $\mathbf{x}_i = [x_{i1} \ x_{i2} \ \dots \ x_{in}]^T \in R^n$  and  $\tau_i = [\tau_{i1} \ \tau_{i2} \ \dots \ \tau_{im}]^T \in R^m$ , a standard SLFN with  $\tilde{N}$  neurons is designed as

$$\sum_{i=1}^{\tilde{N}} \beta_i G(\mathbf{x}_j, \gamma_i, \alpha_i) = \mathbf{o}_j, \quad j = 1, \dots, N \quad (11)$$

where  $\gamma_i = [\gamma_{i1} \ \gamma_{i2} \ \dots \ \gamma_{in}]^T$  is the input weight vector and  $\alpha_i$  is the input bias at  $i$ th hidden node.  $\beta_i = [\beta_{i1} \ \beta_{i2} \ \dots \ \beta_{im}]^T$  is the output weight vector connecting the  $i$ th hidden node and the output node.  $G(\mathbf{x}_j, \gamma_i, \alpha_i)$  is the activation function.

The standard SLFN with  $\tilde{N}$  hidden nodes as shown in Fig. 2 can approximate  $N$  samples with a small error  $\varepsilon$ , which means that  $\sum_{j=1}^N \|\mathbf{o}_j - \tau_j\| < \varepsilon$  if  $\gamma_i, \alpha_i, \beta_i$  exist so that  $H(\mathbf{x}, \gamma, \alpha) \beta \approx \mathbf{T}$

where the hidden layer output matrix is

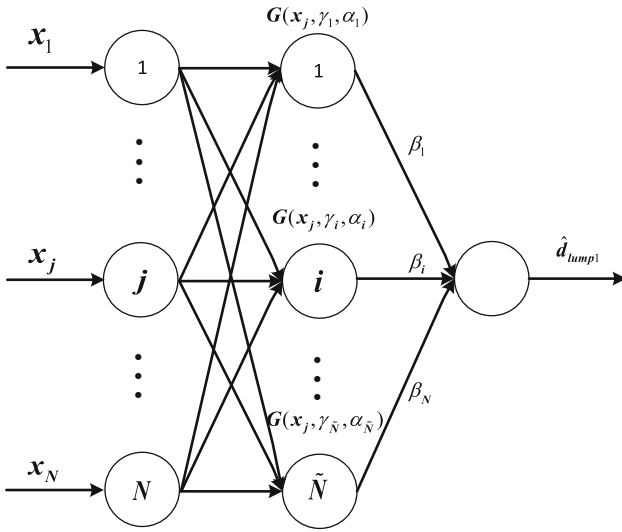


**Fig. 2** The configuration of SLFN with  $\tilde{N}$  neurons

$$\mathbf{H}(\mathbf{x}, \boldsymbol{\gamma}, \boldsymbol{\alpha}) = \begin{bmatrix} G(\mathbf{x}_1, \gamma_1, \alpha_1) & \dots & G(\mathbf{x}_1, \gamma_{\tilde{N}}, \alpha_{\tilde{N}}) \\ \vdots & \dots & \vdots \\ G(\mathbf{x}_N, \gamma_1, \alpha_1) & \dots & G(\mathbf{x}_N, \gamma_{\tilde{N}}, \alpha_{\tilde{N}}) \end{bmatrix} \in R^{N \times \tilde{N}}$$

$$\begin{aligned} \mathbf{x} &= [\mathbf{x}_1 \quad \mathbf{x}_2 \quad \dots \quad \mathbf{x}_N], \quad \boldsymbol{\gamma} = [\gamma_1 \quad \gamma_2 \quad \dots \quad \gamma_{\tilde{N}}], \\ \boldsymbol{\alpha} &= [\alpha_1 \quad \alpha_2 \quad \dots \quad \alpha_{\tilde{N}}], \\ \boldsymbol{\beta} &= [\boldsymbol{\beta}_1^T \quad \boldsymbol{\beta}_2^T \quad \dots \quad \boldsymbol{\beta}_{\tilde{N}}^T]^T \in R^{\tilde{N} \times m}, \quad \text{and} \\ \mathbf{T} &= [\boldsymbol{\tau}_1^T \quad \boldsymbol{\tau}_2^T \quad \dots \quad \boldsymbol{\tau}_N^T]^T \in R^{N \times m}, \end{aligned}$$

The gradient-based back-propagation (BP) algorithm is commonly applied to optimising  $\gamma_i, \alpha_i, \boldsymbol{\beta}_i$  of SLFN. However, there are several drawbacks such as local minima, overfitting, and slow learning rate [24]. Hence, the ELM algorithm is applied to fix the problems based on the following concept.

**Theorem 1** *If the activation function is infinitely differentiable in any interval, then for  $N$  arbitrary distinct samples  $(\mathbf{x}_i, \boldsymbol{\tau}_i) \in R^{n \times m}$ , for any  $\boldsymbol{\gamma}$  and  $\boldsymbol{\alpha}$  randomly chosen from any intervals of  $R^n$  and  $R$  with probability one, the hidden layer output matrix  $\mathbf{H}$  of the SLFN is invertible and  $\|\mathbf{H}\boldsymbol{\beta} - \mathbf{T}\| < \varepsilon$ , where  $\varepsilon$  is any small positive value [24].*

**Remark 2** For pattern classifications, the input weight vector  $\boldsymbol{\gamma}_i$  and the input biases  $\alpha_i$  of ELM-based SLFN are set randomly and independent to the training data. So that the structure of SLFN can be considered as a linear system. Only the output weight matrix  $\boldsymbol{\beta}$  is optimised by calculating the least square solution [24]. Hence, the optimising process is simple and fast. However, for the real time control systems, the least square solution cannot be obtained since the information of  $\mathbf{T}$  is not available. Therefore, the output weight matrix  $\boldsymbol{\beta}$  of ELM is optimised by the adaptive laws

based on Lyapunov criterion [25–28]. The next section presents an adaptive ELM-based STRC to compensate the lumped uncertainty and the nonlinearity of control systems including parameter variations, backlash, Coulomb frictions, and aperiodic disturbances.

### 3.3 Design of ELM-based super-twisting repetitive control (ELMSTRC)

From (2) and (4), the error dynamic can be expressed as

$$\begin{aligned} \ddot{e} &= \ddot{x} - \ddot{r} \\ &= f_o(x) + g_o u + d_{\text{lump}}(x) - \ddot{r} \end{aligned} \quad (13)$$

Based on (10) and (13), the compensated error dynamic can be expressed as

$$\begin{aligned} \ddot{e}_{\text{RC}} &= \ddot{e} + f''_{\text{RC}} \\ &= f_o(x) + g_o u + d_{\text{lump}}(x) - \ddot{r} + f''_{\text{RC}} \\ &= f_o(x) + g_o u + [d_{\text{lump}}(x) + f''_{\text{RC}}] - \ddot{r} \\ &= f_o(x) + g_o u + d_{\text{lump1}}(x) - \ddot{r} \end{aligned} \quad (14)$$

where  $d_{\text{lump1}}(x) = d_{\text{lump}}(x) + f''_{\text{RC}}$  since  $f''_{\text{RC}}$  can be treated as uncertainty during transient. The bounded condition  $|d_{\text{lump1}}(x)| \leq \Delta_{d1}$  is assumed.

In order to estimate the lumped uncertainty  $d_{\text{lump1}}(x)$ , the activation function of neural network is chosen as sigmoidal additive function

$$G(\mathbf{x}, \boldsymbol{\gamma}, \boldsymbol{\alpha}) = \frac{1}{1 + e^{-(\boldsymbol{\gamma} \cdot \mathbf{x} + \boldsymbol{\alpha})}} \quad (15)$$

The actual lumped uncertainty can be expressed as

$$d_{\text{lump1}}(x) = \mathbf{H}\boldsymbol{\beta}^* \quad (16)$$

where  $\boldsymbol{\beta}^*$  is the ideal output weight matrix of the network.

The estimated lumped uncertainty is designed as

$$\hat{d}_{\text{lump1}}(x) = \mathbf{H}\hat{\boldsymbol{\beta}} \quad (17)$$

where  $\hat{\boldsymbol{\beta}}$  is the estimated output weight matrix of the network.

In order to design sliding mode control, the sliding surface is defined as

$$\sigma = \dot{e}_{\text{RC}} + c_1 \ddot{e}_{\text{RC}} \quad (18)$$

where  $c_1 > 0$  is to ensure  $e_{\text{RC}}$  and  $\dot{e}_{\text{RC}}$  asymptotically stable. Then,  $c_1$  is tuned to improve the transient response.

The time derivative of  $\sigma$  is given as

$$\dot{\sigma} = \ddot{e}_{\text{RC}} + c_1 \dot{e}_{\text{RC}} \quad (19)$$

Substituting (14) into (19) yields

$$\begin{aligned} \dot{\sigma} &= f_o(x) + g_o u + d_{\text{lump1}}(x) - \ddot{r} + c_1 \dot{e}_{\text{RC}} \\ &= f_o(x) + g_o u + \hat{d}_{\text{lump1}}(x) + [d_{\text{lump1}}(x) - \hat{d}_{\text{lump1}}(x)] \\ &\quad - \ddot{r} + c_1 \dot{e}_{\text{RC}} \end{aligned} \quad (20)$$

Now, we propose the following control law

$$u = u_1 + u_2 + u_3 \quad (21)$$

where the super-twisting control is designed as

$$u_1 = g_0^{-1}$$

$$\left[ -\lambda_1 |\sigma|^{\frac{1}{2}} \text{sign}(\sigma) - \int_0^t \lambda_2 \text{sign}(\sigma(\tau)) d\tau + \ddot{r} - c_1 \dot{e}_{RC} - f_o(x) \right] \quad (22)$$

In addition, the exponential reaching law [30] is designed as

$$u_2 = g_0^{-1} [-\Psi_1 \text{sign}(\sigma) - \Psi_2 \sigma] \quad (23)$$

to ensure fast convergence of sliding variable and reduced chattering. For the gain selection criteria, if  $\Psi_1$  is increased, then  $\Psi_2$  is decreased.

The lumped uncertainty compensation signal is designed as

$$u_3 = g_0^{-1} [-\hat{d}_{lump1}(x)] \quad (24)$$

The estimated output weight matrix  $\hat{\beta}$  is updated by the following adaptive law

$$\dot{\hat{\beta}}^T = \eta \sigma H \quad (25)$$

where  $\eta > 0$  is positive adaptive gain.

So that the ideal output weight matrix  $\beta^*$  can be adaptively estimated in the closed-loop system.

**Theorem 2** *The ELMSTRC system under the control of (21) is stable if the following conditions are satisfied.*

- (a)  $s + c_1$  is Hurwitz stable polynomial.
- (b) The derivative of Lyapunov function is  $\dot{L} \leq 0$ .

**Proof** Condition (a) is satisfied since  $c_1 > 0$ , and the root of  $s + c_1 = 0$  is in left hand side of complex plane.

Substituting (21) into (20) yields

$$\begin{aligned} \dot{\sigma} &= f_o(x) + g_o[u_1 + u_2 + u_3] \\ &\quad + \hat{d}_{lump1}(x) + [d_{lump1}(x) - \hat{d}_{lump1}(x)] - \ddot{r} + c_1 \dot{e}_{RC} \\ \dot{\sigma} &= f_o(x) + g_o g_0^{-1} \left[ -\lambda_1 |\sigma|^{\frac{1}{2}} \text{sign}(\sigma) - \int_0^t \lambda_2 \text{sign}(\sigma(\tau)) d\tau \right. \\ &\quad \left. + \ddot{r} - c_1 \dot{e}_{RC} - f_o(x) - \Psi_1 \text{sign}(\sigma) - \Psi_2 \sigma - \hat{d}_{lump1}(x) \right] \\ &\quad + \hat{d}_{lump1}(x) + H \tilde{\beta} - \ddot{r} + c_1 \dot{e}_{RC} \\ \dot{\sigma} &= -\lambda_1 |\sigma|^{\frac{1}{2}} \text{sign}(\sigma) - \int_0^t \lambda_2 \text{sign}(\sigma(\tau)) d\tau - \Psi_1 \text{sign}(\sigma) \\ &\quad - \Psi_2 \sigma + H \tilde{\beta} \end{aligned} \quad (26)$$

$$\begin{aligned} \text{where } d_{lump1}(x) - \hat{d}_{lump1}(x) &= H \beta^* - H \tilde{\beta} = H [\beta^* - \tilde{\beta}] \\ &= H \tilde{\beta}. \end{aligned}$$

Define the Lyapunov function as

$$L = \frac{1}{2} \sigma^2 + \frac{1}{2\eta} \tilde{\beta}^T \tilde{\beta} \quad (27)$$

where  $\eta > 0$ .

Substituting (26) into the derivative of (27) yields

$$\begin{aligned} \dot{L} &= \sigma \dot{\sigma} + \frac{1}{\eta} \tilde{\beta}^T \tilde{\beta} \\ &= \sigma \left[ -\lambda_1 |\sigma|^{\frac{1}{2}} \text{sign}(\sigma) - \int_0^t \lambda_2 \text{sign}(\sigma(\tau)) d\tau - \Psi_1 \text{sign}(\sigma) - \Psi_2 \sigma + H \tilde{\beta} \right] \\ &\quad + \frac{1}{\eta} \dot{\tilde{\beta}}^T \tilde{\beta} = \left[ \sigma H + \frac{1}{\eta} \dot{\tilde{\beta}}^T \right] \tilde{\beta} \\ &\quad + \sigma \left\{ -\lambda_1 |\sigma|^{\frac{1}{2}} \text{sign}(\sigma) - \int_0^t \lambda_2 \text{sign}(\sigma(\tau)) d\tau - \Psi_1 \text{sign}(\sigma) - \Psi_2 \sigma \right\} \end{aligned}$$

With the adaptive law (25) and the constant ideal output weight matrix  $\beta^*$ :

$$\dot{\tilde{\beta}}^T = \dot{\beta}^{*T} - \dot{\tilde{\beta}}^T = 0 - \eta \sigma H = -\eta \sigma H \quad (28)$$

So that

$$\begin{aligned} \dot{L} &= \sigma \left\{ -\lambda_1 |\sigma|^{\frac{1}{2}} \text{sign}(\sigma) - \int_0^t \lambda_2 \text{sign}(\sigma(\tau)) d\tau - \Psi_1 \text{sign}(\sigma) - \Psi_2 \sigma \right\} \\ \dot{L} &= -\lambda_1 |\sigma|^{\frac{3}{2}} - \lambda_2 |\sigma| t - \Psi_1 |\sigma| - \Psi_2 \sigma^2 \end{aligned} \quad (29)$$

By selecting the positive gains  $\lambda_1 > 0$ ,  $\lambda_2 > 0$ ,  $\Psi_1 > 0$ , and  $\Psi_2 > 0$ . So that we can achieve  $\dot{L} \leq 0$  and condition (b) is satisfied.  $\square$

**Remark 3** During the reaching phase, the two parameters  $\lambda_1$  and  $\lambda_2$  are optimised based on the robust exact differentiation method [31] to ensure  $\sigma$  and  $\dot{\sigma}$  converging to zero in finite time. During the sliding phase  $\sigma = \dot{\sigma} = 0$ ,  $c_1$  is tuned to ensure the RC compensated error  $e_{RC}$  and  $\dot{e}_{RC}$  converging to zero asymptotically. Finally,  $\omega_q$  in RC low-pass filter is tuned to ensure the tracking error  $e$  converging to zero.

**Remark 4** The conventional SMC produces undesired chattering due to the discontinuity of sign function. Hence, the proposed controller applies STC algorithm and generates continuous signal. So that the chattering can be reduced.

**Remark 5** During the reaching phase, the two parameters  $\Psi_1$  and  $\Psi_2$  are optimised based on the exponential reaching law [30] to ensure fast convergence and less chattering. The two parameters  $\Psi_1$  and  $\Psi_2$  are tuned oppositely to minimise the trade-off between the convergence rate and chattering.

## 4 Simulation and comparison studies

In the simulations, a model of industrial plant emulator with DC servo motor [32] is considered.

The plant model of system with full loads on both drive disk and load disk (Moment of inertia :  $J = 0.0675 \text{ kg m}^2$ ) is provided in (1) as follows:

$$\ddot{x} = f(x) + g(x)[u + d] \quad (30)$$

where the nominal plant parameters are set as:  $g(x) = g_o = 344.2963$ ,  $f(x) = f_o(x) = -13.5308\dot{x}$  and the disturbance is set as zero:  $d = 0$ .

The sampling period is set to be 0.001768 s.

In ELMSTRC design, the initial input weight  $\gamma$  and input bias  $\alpha$  are chosen randomly within the intervals  $[-1, 1]$  and  $[0, 1]$ , respectively. The number of ELM inputs and that of neurons are chosen as  $N = 2$  and  $\tilde{N} = 25$ , respectively. So the input vector of ELM is  $x = [x_1 \ x_2]^T = [x \ \dot{x}]^T$ . The parameter of adaptive law (28) is chosen as  $\eta = 10,000$ . So that the condition in Theorem 1 is satisfied. Then, we apply control law (21) with parameters  $c_1 = 5$ ,  $\lambda_1 = 100$ ,  $\lambda_2 = 20$ ,  $\Psi_1 = 40$ , and  $\Psi_2 = 40$ . The repetition period of RC is  $T_p = 3.6209$  s. The cut-off frequency of RC low-pass filter is set to be 10 Hz. So that all the conditions in Theorem 2 are satisfied.

A 0.2762 Hz triangle signal (31) as shown in Fig. 3 is defined as reference input  $r$  of simulation.

$$r = \int_0^\infty \operatorname{sgn}(\cos(2\pi(0.2762)t))dt \quad (31)$$

Then, MATLAB/Simulink is utilised to simulate the tracking errors  $e$  of various controllers for tracking the reference input. In the simulation, the root mean square (RMS) value of  $e$  is analysed for clarity.

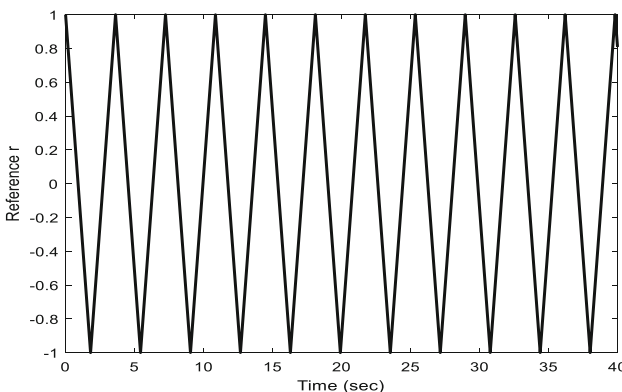


**Fig. 3** Triangle reference signal  $r$

### 4.1 Tracking performance of periodic signals with viscous friction

The tracking errors  $e$  of STRC, ELMSTC, and proposed ELMSTRC are analysed as shown in Fig. 4. Figure 4 shows that ELMSTRC has a better tracking accuracy in steady state, since ELMSTRC can reduce the tracking error by 38% compared to ELMSTC and 74% compared to STRC. Therefore, ELMSTRC has a better performance in tracking periodic signal and compensating viscous friction.

### 4.2 Tracking performance of periodic signals with aperiodic disturbance

Three types of aperiodic disturbances (32) as shown in Fig. 5a–c are applied at the input of plant model (30) as follows:

$$d = \begin{cases} d_1 = 0.15 \tanh(t - 20) - 0.15 \tanh(t - 27) \\ d_2 = \text{step disturbance} \\ d_3 = \text{ramp disturbance} \end{cases} \quad (32)$$

The tracking errors  $e$  of RC, STRC, and proposed ELMSTRC are analysed as shown in Fig. 6a–c. Figure 6a–c shows that ELMSTRC can compensate the impulse disturbance, step disturbance, and ramp disturbance effectively, since ELMSTRC can reduce the tracking error by 77%, 73%, and 74%, respectively, compared to STRC and 89%, 87%, and 87%, respectively, compared to RC. Therefore, ELMSTRC is robust to aperiodic uncertainty.

### 4.3 Tracking performance of periodic signals with nonlinear friction

A Coulomb friction  $f_c(x)$  is applied to the plant model (30) so that

$$f(x) = f_o(x) + f_c(x) \quad (33)$$

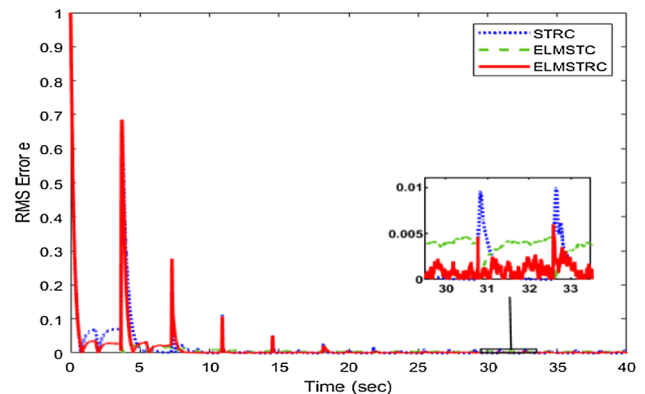
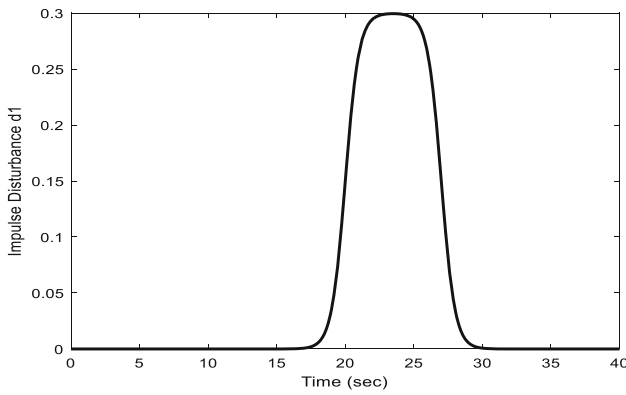
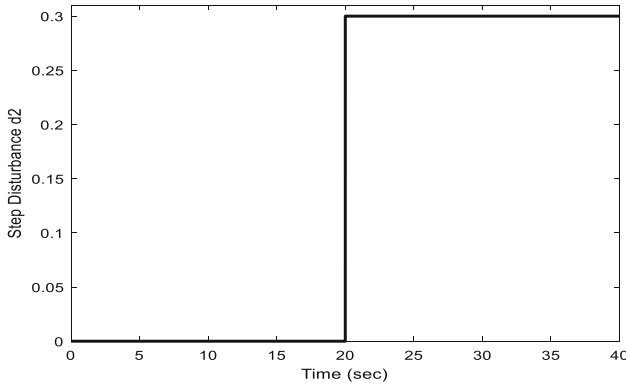


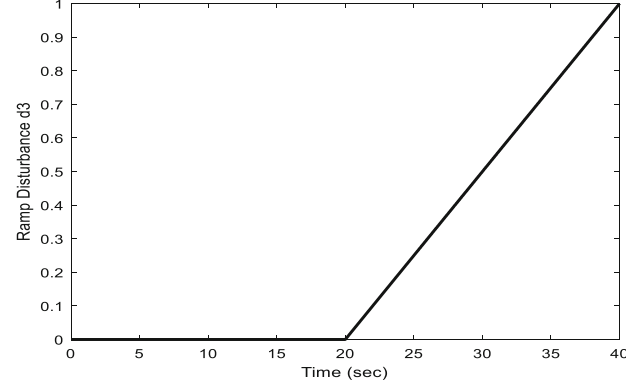
**Fig. 4** Tracking errors of STRC, ELMSTC, and ELMSTRC with viscous friction and triangle reference



(a)



(b)

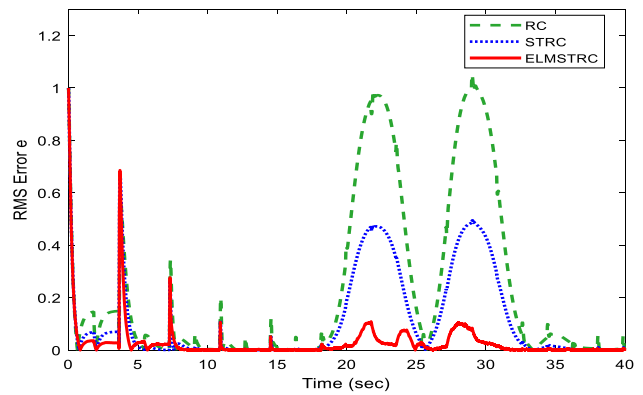


(c)

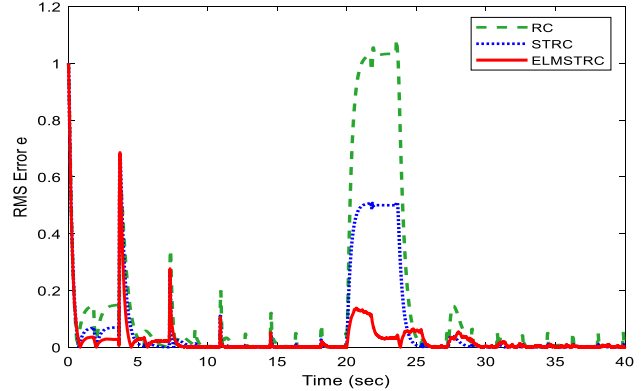
**Fig. 5** Aperiodic disturbances  $d$ : **a** impulse disturbance  $d_1$ , **b** step disturbance  $d_2$ , **c** ramp disturbance  $d_3$

where  $f_c(x) = -68.8593\text{sign}[\dot{x}]$ .

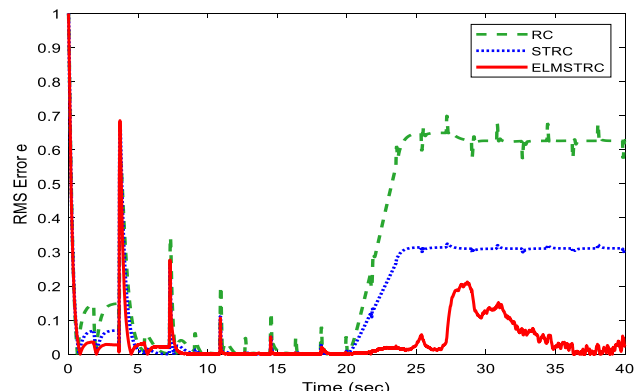
Then, the tracking errors  $e$  of RC, STRC, and proposed ELMSTRC are analysed as shown in Fig. 7. Figure 7 demonstrates that ELMSTRC has a less tracking error in steady state, since ELMSTRC can improve the tracking accuracy by 88% compared to STRC and 95% compared to RC. Therefore, ELMSTRC has a better performance in compensating nonlinear friction.



(a)



(b)



(c)

**Fig. 6** Tracking errors of RC, STRC, and ELMSTRC with **a** impulse disturbance  $d_1$ , **b** step disturbance  $d_2$ , **c** ramp disturbance  $d_3$

#### 4.4 Tracking performance of periodic signals with backlash

A backlash model  $g_b(x)$  [13] with 50 rad of deadband width is placed at the input of plant model (30) so that

$$g(x) = g_b(x)g_o \quad (34)$$

$$\text{where } g_b(x) = \begin{cases} x - d & x > d \\ 0 & |x| < d \\ x + d & x < -d \end{cases}, d = 50 \text{ rad.}$$

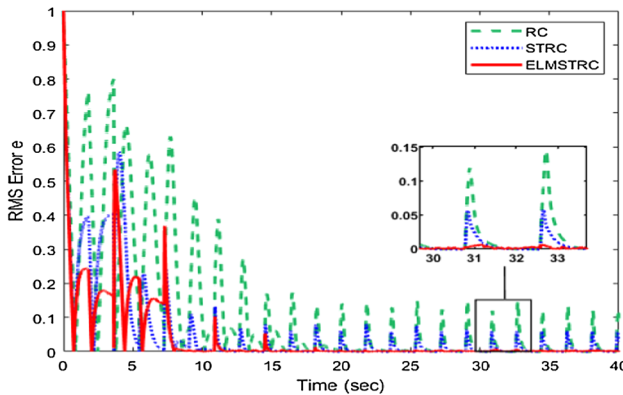


**Fig. 7** Tracking errors of RC, STRC, and ELMSTRC with Coulomb friction and triangle reference

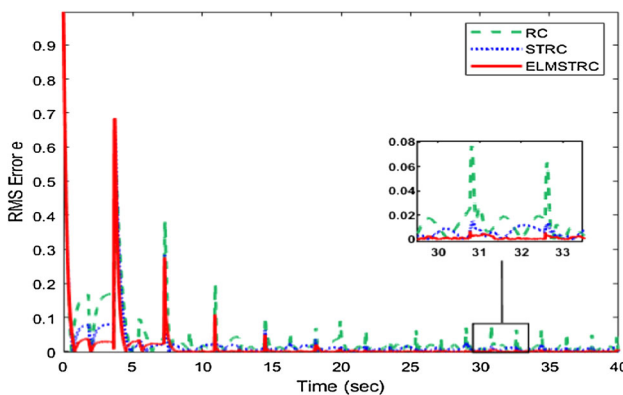


**Fig. 8** Tracking errors of RC, STRC, and ELMSTRC with backlash and triangle reference

Then, the tracking errors  $e$  of RC, STRC, and proposed ELMSTRC are analysed as shown in Fig. 8. Figure 8 shows that ELMSTRC has a better tracking accuracy in steady state, since ELMSTRC can reduce the tracking error by 54% compared to STRC, and 91% compared to RC. Therefore, ELMSTRC has a better performance in compensating backlash.

#### 4.5 Tracking performance of periodic signals with parameter uncertainty

The tracking errors  $e$  of RC, STRC, and proposed ELMSTRC are analysed in the conditions of Case 1 (four brass weights of 0.2 kg each on drive disk and 0.5 kg each on load disk), Case 2 (four brass weights of 0.5 kg each on drive disk and 0.2 kg each on load disk), and Case 3 (four brass weights of 0.5 kg each on drive disk and no brass weights on load disk). The details of case studies for parameter uncertainty are shown in Table 1 where  $J$ —moment of inertia,  $n_{pd}$ —number of teeth on bottom pulley,  $n_{pl}$ —number of teeth on top pulley,  $m_{wd}$ —mass of brass

weights on drive disk,  $r_{wd}$ —radius from centre of plate on drive disk,  $m_{wl}$ —mass of brass weights on load disk, and  $r_{wl}$ —radius from centre of plate on load disk.

In Fig. 9a–c, the tracking performance of RC is varying from Case 1 to Case 3 with the lowest tracking accuracy. Therefore, RC cannot compensate the load uncertainty. The tracking performance of STRC is unchanged for all cases with higher tracking accuracy. Therefore, STRC can compensate the load uncertainty. The tracking performance of ELMSTRC is unchanged for all cases with highest tracking accuracy. Therefore, ELMSTRC is robust against the load variation.

#### 4.6 Chattering reduction

For chattering comparison, the tracking errors  $e$  of sliding mode-based repetitive control (SMRC) [4], and proposed ELMSTRC are analysed in the simulations.

From the simulation results in Fig. 10, the proposed ELMSTRC has a less tracking error and less chattering compared to SMRC.

#### 4.7 Tracking performance, space cost and time cost comparison with other machine learning algorithm

In order to demonstrate the significance of the proposed algorithm, the tracking errors of the RBFNN-based STRC, and the proposed ELM-based STRC are analysed in Fig. 11 and Table 2, where ELM-based STRC has a less tracking error in steady state compared to RBFNN-based STRC. Therefore, the proposed ELM-based STRC has a better tracking performance over other machine learning algorithm.

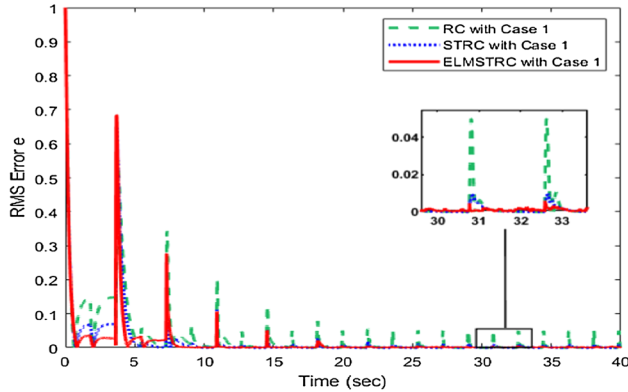
The space cost and time cost comparisons of RBFNN-based STRC, and ELM-based STRC are shown in Tables 3 and 4, respectively, where the RBFNN-based STRC has a higher space cost and time cost due to the large number of tuning parameters. The ELM-based STRC has a less time cost while the space cost is similar to the RBFNN-based STRC.

#### 4.8 The tracking accuracy under different random intervals of input weight and input bias

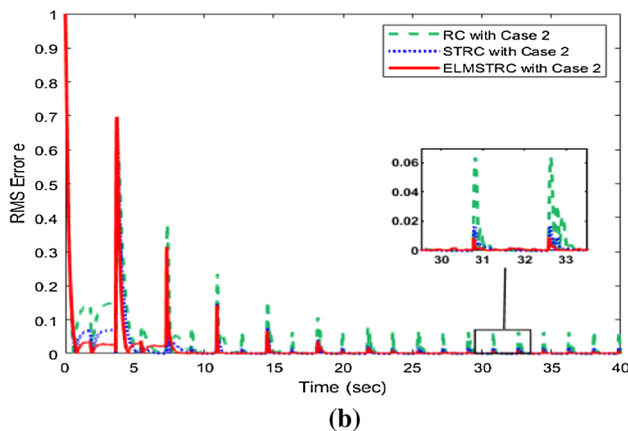
In order to test the effects of input weight and input bias on the tracking accuracy, the tracking errors of the proposed ELM-based STRC with different random intervals are analysed in Table 5. The simulation results in Table 5 show that the random intervals of input weight and input bias do not affect the tracking performance of ELM-based STRC.

**Table 1** Details of case studies for parameter uncertainty

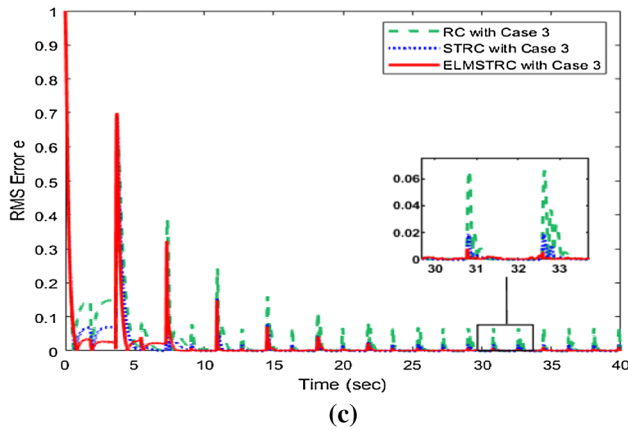
Case studies	$n_{pd}$	$n_{pl}$	$m_{wd}$ (kg)	$r_{wd}$ (m)	$m_{wl}$ (kg)	$r_{wl}$ (m)	$J$ ( $\text{kg m}^2$ )
Case 1	24	36	0.8	0.05	2	0.1	0.0675
Case 2	24	36	2	0.05	0.8	0.1	0.1033
Case 3	24	36	2	0.05	0	0.1	0.1114



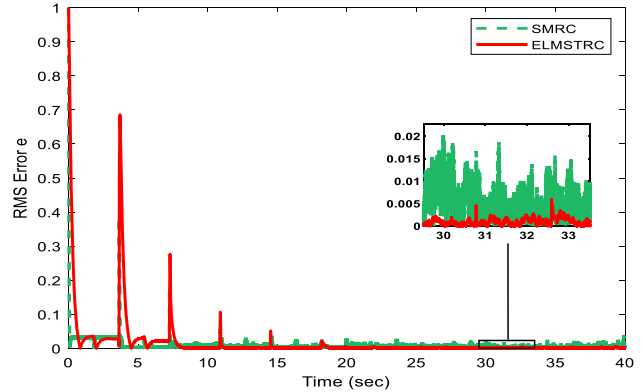
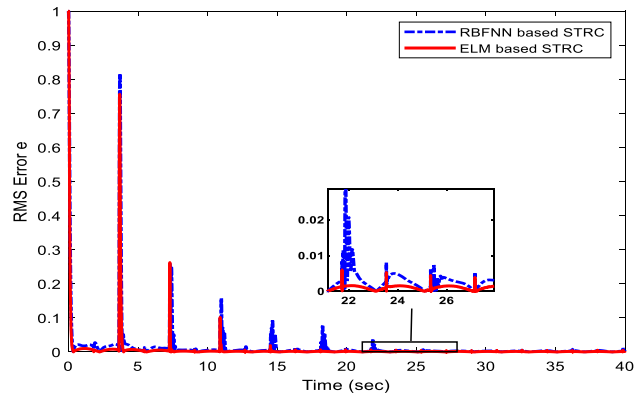
(a)



(b)



(c)

**Fig. 9** Tracking errors of **a** RC, STRC, and ELMSTRC with Case 1, **b** RC, STRC, and ELMSTRC with Case 2, **c** RC, STRC, and ELMSTRC with Case 3 with a triangle reference**Fig. 10** Tracking errors of SMRC and ELMSTRC with a triangle reference**Fig. 11** Tracking errors of RBFNN-based STRC, and ELM-based STRC with a triangle reference**Table 2** Comparison of tracking errors (RBFNN-based STRC and ELM-based STRC)

Control	RBFNN-based STRC	ELM-based STRC
Error	0.0050	0.0015

## 5 Experiment and comparison studies

In the experiment, the positioning control of ECP Model 220 Industrial Plant Emulator [32] with brushless DC servo motor is considered (Figs. 12 and 13).

The rigid body plant with full loads on drive disk and load disk provided in the manual of ECP [32] is used to test

**Table 3** Comparison of space cost (RBFNN-based STRC and ELM-based STRC)

Control	RBFNN-based STRC	ELM-based STRC
Parameter size	1251	1251

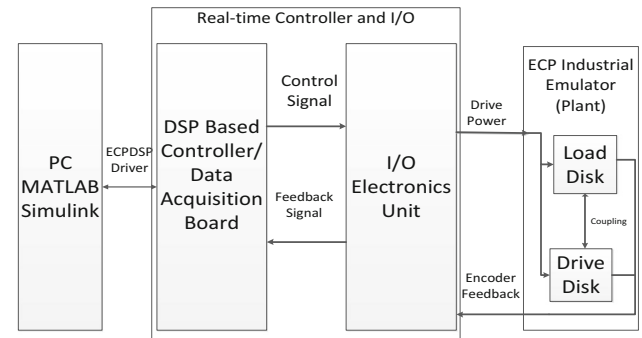
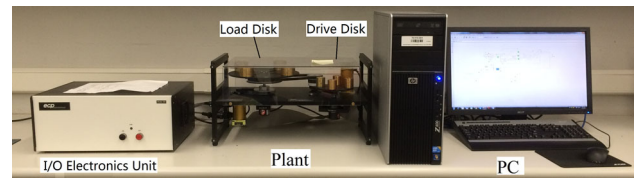
the proposed control algorithm. The plant can be modelled as a simple rigid body with viscous friction. The sampling period is set to be 0.001768 s.

In ELMSTRC design, the initial input weight  $\gamma$  and input bias  $\alpha$  are chosen randomly within the intervals  $[-1, 1]$  and  $[0, 1]$ , respectively. The number of ELM inputs and neurons are chosen as  $N = 2$  and  $\tilde{N} = 25$ , respectively. Then, we apply control law (21) with parameters  $f_o(x) = -13.5308x$ ,  $g_o = 344.2963$ ,  $c_1 = 5$ ,  $\lambda_1 = 2400$ ,  $\lambda_2 = 4000$ ,  $\Psi_1 = 10$  and  $\Psi_2 = 10$ , as well as adaptive law (28) with parameter  $\eta = 25.7143$ . The repetition period of RC is  $T_p = 3.6209$  s. The cut-off frequency of RC low-pass filter is set to be 10 Hz. So that all the conditions in Theorems 1 and 2 are satisfied.

The reference input  $r$  is set as a triangle signal (31) as shown in Fig. 3 in the experiment. Then, MATLAB/Simulink is utilised to analyse the RMS tracking errors  $e$  of various controllers for tracking the reference input.

### 5.1 Tracking performance of periodic signals with viscous friction

The tracking errors  $e$  of ELMSTC and proposed ELMSTRC are analysed as shown in Fig. 14. Figure 14 shows that ELMSTRC has a less tracking error in steady state, since ELMSTRC can improve the tracking accuracy by 53% compared to ELMSTC. Therefore, ELMSTRC has

**Fig. 12** Block diagram of the experimental system**Fig. 13** Hardware setup of the experimental system

a better performance in tracking periodic signal, and compensating viscous friction.

### 5.2 Tracking performance of periodic signals with nonlinear friction

A friction clamp is applied on the load disk to generate Coulomb friction. Then, the tracking errors  $e$  of proposed ELMSTRC and RC are analysed as shown in Fig. 15. Figure 15 demonstrates that ELMSTRC has a better tracking accuracy in steady state, since ELMSTRC can reduce the tracking error by 44% compared to RC. Therefore, ELMSTRC has a better performance in compensating nonlinear friction.

**Table 4** Comparison of time cost (RBFNN-based STRC and ELM-based STRC)

Control	Uncertainty	RBFNN-based STRC	ELM-based STRC
Prediction time (unit: second)			
Viscous friction	25.6	14.6	
Coulomb friction	5.7	4.4	
Backlash	25.5	14.5	

**Table 5** The tracking performances of the proposed ELM-based STRC under different intervals of input weight and input bias

Input intervals of $\gamma$ ( $\alpha \in [0, 1]$ )	Error	Input intervals of $\alpha$ ( $\gamma \in [-1, 1]$ )	Error
[-0.5, 0.5]	0.0158	[0, 0.5]	0.0158
[-1, 1]	0.0160	[0, 1]	0.0160
[-2, 2]	0.0157	[0, 2]	0.0159
[-3, 3]	0.0160	[0, 3]	0.0160
[-4, 4]	0.0160	[0, 4]	0.0163

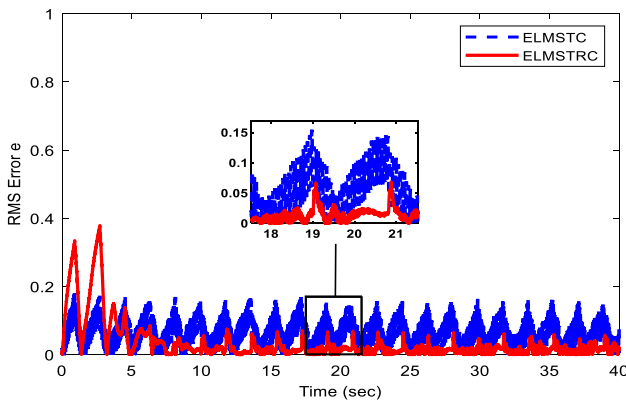


**Fig. 14** Tracking errors of ELMSTC and ELMSTRC with viscous friction and triangle reference

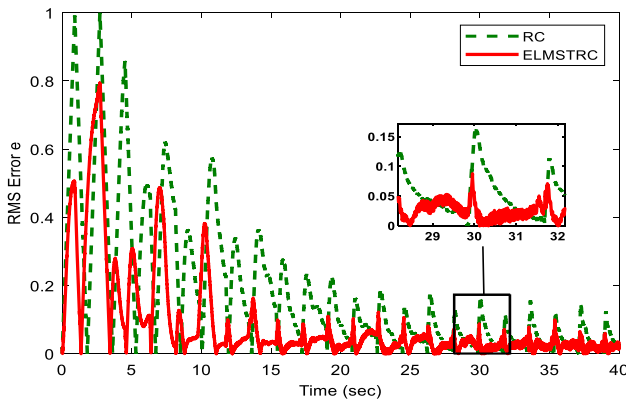


**Fig. 15** Tracking errors of RC and ELMSTRC with Coulomb friction and triangle reference

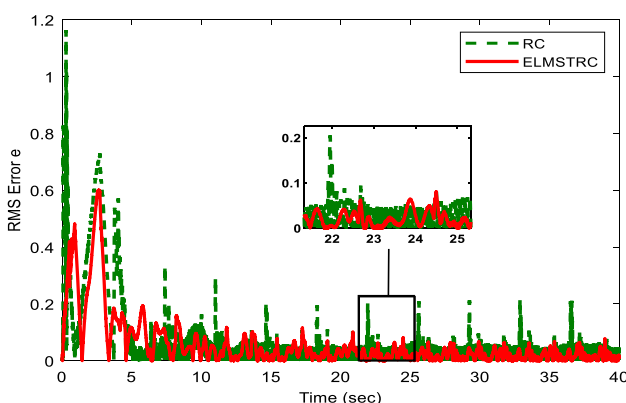
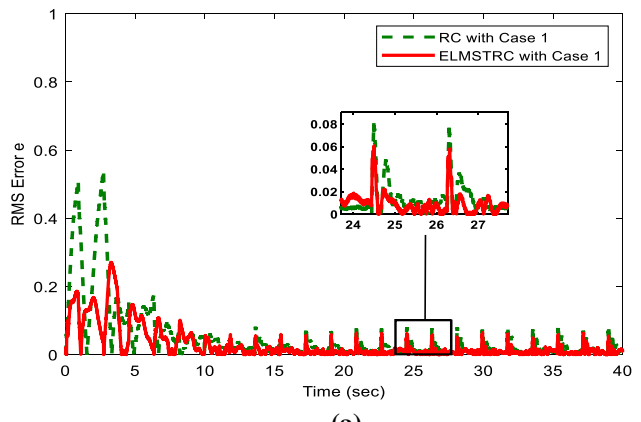


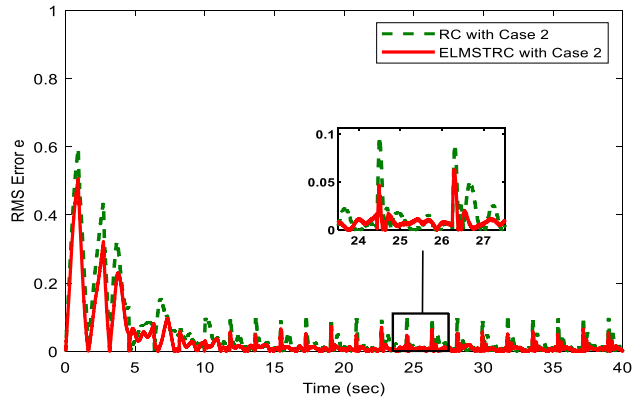
**Fig. 16** Tracking errors of RC and ELMSTRC with backlash and triangle reference

### 5.3 Tracking performance of periodic signals with backlash

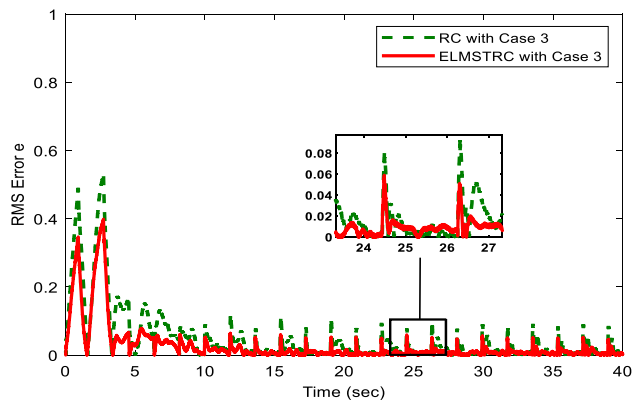
The screw between the top pulley and the bottom pulley is unscrewed to generate backlash. Then, the tracking errors  $e$  of proposed ELMSTRC and RC are analysed as shown in



**(a)**



**(b)**



**(c)**

**Fig. 17** Tracking errors of **a** RC and ELMSTRC with Case 1, **b** RC and ELMSTRC with Case 2, **c** RC and ELMSTRC with Case 3 with a triangle reference

Fig. 16. Figure 16 shows that ELMSTRC has a less tracking error in steady state, since ELMSTRC can improve the tracking accuracy by 60% compared to RC. Therefore, ELMSTRC has a better performance in compensating backlash.

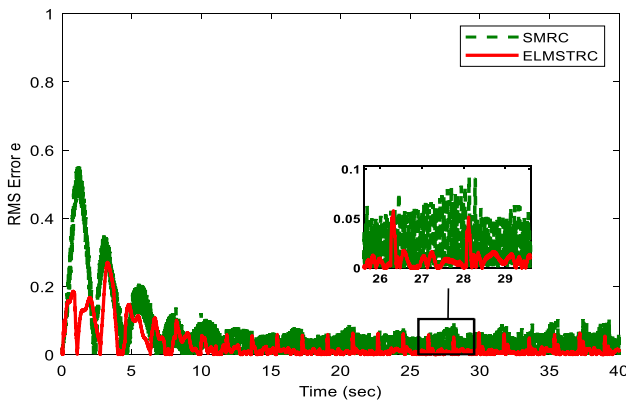


**Fig. 18** Tracking errors of SMRC and ELMSTRC with a triangle reference

#### 5.4 Tracking performance of periodic signals with parameter uncertainty

The tracking errors  $e$  of RC and proposed ELMSTRC are analysed in the conditions of Case 1 (four brass weights of 0.2 kg each on drive disk and 0.5 kg each on load disk), Case 2 (four brass weights of 0.5 kg each on drive disk and 0.2 kg each on load disk), and Case 3 (four brass weights of 0.5 kg each on drive disk and no brass weights on load disk). The details of case studies for parameter uncertainty are shown in Table 1.

In Fig. 17a–c, the tracking performance of RC is varying from Case 1 to Case 3. Therefore, RC is not robust against the load variation. The tracking performance of ELMSTRC is unchanged for all cases. Therefore, ELMSTRC can compensate the load uncertainty with less tracking error.

#### 5.5 Chattering reduction

The tracking errors  $e$  of SMRC [4] and proposed ELMSTRC are analysed in the experiment.

From the experimental results in Fig. 18, the proposed ELMSTRC has a better tracking accuracy with less chattering compared to SMRC.

### 6 Conclusions

In conclusion, the extreme learning machine-based super-twisting repetitive control has been proposed to improve the performance of tracking periodic signals, as well as compensating the viscous friction and nonlinear friction. Moreover, ELMSTRC can compensate the aperiodic disturbance, backlash, and parameter uncertainty. The stability criteria have been derived. The significances of the proposed algorithm have been demonstrated through

simulations and experiments on a brushless DC servo motor. The comparison studies show that the proposed ELMSTRC has an excellent performance in tracking periodic signal, aperiodic disturbance compensation, friction compensation, and backlash compensation, as well as robustness against the system uncertainty. In the future, improved error correction-based neural network control [33] will be considered to improve the tracking accuracy, transient speed, and robustness of RC system.

#### Compliance with ethical standards

**Conflict of interest** The authors declare that they have no conflict of interest.

#### References

1. Inoue T, Nakano M, Iwai S (1981) High accuracy control of a proton synchrotron magnet power supply. In: Proceedings of 8th world congress IFAC, Kyoto, August 1981, pp 3137–3142
2. Francis BA, Wonham WM (1975) The internal model principle for linear multivariable regulators. *Appl Math Optim* 2(2):170–194
3. Hara S, Yamamoto Y, Omata T, Nakano M (1988) Repetitive control system: a new type servo system for periodic exogenous signals. *IEEE Trans Autom Control* 33(7):659–666
4. Chen S, Lai YM, Tan SC, Tse CK (2009) Fast response low harmonic distortion control scheme for voltage source inverters. *IET Power Electron* 2(5):574–584. <https://doi.org/10.1049/iet-pel.2008.0149>
5. Kurniawan E, Cao Z, Man Z (2014) Design of robust repetitive control with time-varying sampling periods. *IEEE Trans Industr Electron* 61(6):2834–2841. <https://doi.org/10.1109/TIE.2013.2276033>
6. Sayem AHM, Cao Z, Man Z (2017) Model free ESO-based repetitive control for rejecting periodic and aperiodic disturbances. *IEEE Trans Industr Electron* 64(4):3433–3441. <https://doi.org/10.1109/TIE.2016.2606086>
7. Chuei R, Cao Z, Man Z (2017) Super twisting observer based repetitive control for aperiodic disturbance rejection in a brushless DC servo motor. *Int J Control Autom Syst*. <https://doi.org/10.1007/s12555-016-0415-x>
8. Hamza MF, Yap HJ, Choudhury IA, Chiroma H, Kumbasar T (2018) A survey on advancement of hybrid type 2 fuzzy sliding mode control. *Neural Comput Appl* 30(2):331–353. <https://doi.org/10.1007/s00521-017-3144-z>
9. Yuan X, Yang Y, Wang H, Wang Y (2013) Genetic algorithm-based adaptive fuzzy sliding mode controller for electronic throttle valve. *Neural Comput Appl* 23(1):209–217. <https://doi.org/10.1007/s00521-012-1327-1>
10. Hsu C-F, Kao W-F (2018) Perturbation wavelet neural sliding mode position control for a voice coil motor driver. *Neural Comput Appl*. <https://doi.org/10.1007/s00521-018-3413-5>
11. Levant A (1993) Sliding order and sliding accuracy in sliding mode control. *Int J Control* 58(6):1247–1263. <https://doi.org/10.1080/00207179308923053>
12. Chuei R, Cao Z, Man Z (2016) Design of super twisting repetitive control. In: 2016 IEEE 11th conference on industrial electronics

- and applications (ICIEA), 5–7 June 2016, pp 758–762. <https://doi.org/10.1109/iciea.2016.7603683>
13. Nordin M, Gutman PO (2002) Controlling mechanical systems with backlash—a survey. *Automatica* 38(10):1633–1649. [https://doi.org/10.1016/S0005-1098\(02\)00047-X](https://doi.org/10.1016/S0005-1098(02)00047-X)
  14. Coulomb damping. [https://en.wikipedia.org/wiki/Coulomb\\_damping](https://en.wikipedia.org/wiki/Coulomb_damping). Accessed 14 Sept 2017
  15. Acho L, Iurian C, Ikhouane F, Rodellar J (2007) Robust-adaptive control of mechanical systems with friction: application to an industrial emulator. In: Proceedings of 2007 American control conference, 9–13 July 2007, pp 5970–5974. <https://doi.org/10.1109/acc.2007.4282379>
  16. Cai M, Xiang Z (2018) Adaptive finite-time control of a class of non-triangular nonlinear systems with input saturation. *Neural Comput Appl* 29(7):565–576. <https://doi.org/10.1007/s00521-016-2540-0>
  17. Li Y, Tong S, Li T (2013) Adaptive fuzzy output feedback control of nonlinear uncertain systems with unknown backlash-like hysteresis based on modular design. *Neural Comput Appl* 23(1):261–270. <https://doi.org/10.1007/s00521-013-1355-5>
  18. Çetin M, Bahtiyar B, Beyhan S (2019) Adaptive uncertainty compensation-based nonlinear model predictive control with real-time applications. *Neural Comput Appl* 31(2):1029–1043. <https://doi.org/10.1007/s00521-017-3068-7>
  19. Liu J (2013) Radial basis function (RBF) neural network control for mechanical systems: design, analysis and matlab simulation. Springer, Berlin
  20. Wang H, Xu Z, Do MT, Zheng J, Cao Z, Xie L (2015) Neural-network-based robust control for steer-by-wire systems with uncertain dynamics. *Neural Comput Appl* 26(7):1575–1586. <https://doi.org/10.1007/s00521-014-1819-2>
  21. Eski İ, Yıldırım Ş (2017) Neural network-based fuzzy inference system for speed control of heavy duty vehicles with electronic throttle control system. *Neural Comput Appl* 28(1):907–916. <https://doi.org/10.1007/s00521-016-2362-0>
  22. Yan H, Li Y (2017) Adaptive NN prescribed performance control for nonlinear systems with output dead zone. *Neural Comput Appl* 28(1):145–153. <https://doi.org/10.1007/s00521-015-2043-4>
  23. Cortes C, Vapnik V (1995) Support-vector networks. *Mach Learn* 20(3):273–297. <https://doi.org/10.1007/bf00994018>
  24. Huang G-B, Zhu Q-Y, Siew C-K (2006) Extreme learning machine: theory and applications. *Neurocomputing* 70(1):489–501. <https://doi.org/10.1016/j.neucom.2005.12.126>
  25. Rong H-J, Zhao G-S (2013) Direct adaptive neural control of nonlinear systems with extreme learning machine. *Neural Comput Appl* 22(3):577–586. <https://doi.org/10.1007/s00521-011-0805-1>
  26. Yang Y, Wang Y, Yuan X, Chen Y, Tan L (2013) Neural network-based self-learning control for power transmission line deicing robot. *Neural Comput Appl* 22(5):969–986. <https://doi.org/10.1007/s00521-011-0789-x>
  27. Yang C, Huang K, Cheng H, Li Y, Su C (2017) Haptic Identification by ELM-controlled uncertain manipulator. *IEEE Trans Syst Man Cybern: Syst* 47(8):2398–2409. <https://doi.org/10.1109/TSMC.2017.2676022>
  28. Hu Y et al (2019) Extreme-learning-machine-based FNTSM control strategy for electronic throttle. *Neural Comput Appl*. <https://doi.org/10.1007/s00521-019-04446-9>
  29. Doh TY, Ryoo JR, Chung MJ (2006) Design of a repetitive controller: an application to the track-following servo system of optical disk drives. *IEE Proc Control Theory Appl* 153(3):323–330
  30. Liu J, Wang X (2011) Advanced sliding mode control for mechanical systems. Springer, Berlin
  31. Levant A (1998) Robust exact differentiation via sliding mode technique. *Automatica* 34(3):379–384
  32. Manual For Model 220 Industrial Emulator/Servo Trainer (1995), 2.3 edn. Educational Control Products, Bell Canyon, CA
  33. Meng X, Rozycski P, Qiao J, Wilamowski BM (2018) Nonlinear system modeling using RBF networks for industrial application. *IEEE Trans Ind Inf* 14(3):931–940. <https://doi.org/10.1109/TII.2017.2734686>

**Publisher's Note** Springer Nature remains neutral with regard to jurisdictional claims in published maps and institutional affiliations.